



PROBA 2 - LYRA

Final calibration PTB-Bessy II

Doc. Reference

Date:

Issue:

Page: 1 of 27

Pre-Analysis Report

Final calibration NI beamline (40-240nm)

PROBA-2 / LYRA

20-31 March 2006

Doc. RP-ROB-LYR-0132-NI-March2006

issue Version 1.0

30 May 2006

Prepared by : A. BEN MOUSSA (ROB)

Verified by :

Released by :



PROBA 2 - LYRA
Final calibration PTB-Bessy II

Doc. Reference
Date:
Issue:
Page: 2 of 27

Distribution List

Recipients	Affiliation	Nr. of Copies
LYRA team	CSL, IMO, PMOD, MPS, IEMN, ROB	Email copy

Document Change Record

Issue	Date	Comments
1.0	30/06/2006	Initial issue



Table of Contents

<i>Scope</i>	4
1 Execution Plan for LYRA	4
2 RESULTS	5
2.1 Channel 1-1 (Head 1 ; Channel 1: Ly- α , MSM12)	5
2.2 Channel 1-2 (Head 1 ; Channel 2: Herzberg, PIN10)	7
2.3 Channel 1-3 (Head 1 ; Channel 3: Al, MSM11)	9
2.4 Channel 2-1 (Head 2 ; Channel 1: Ly- α , MSM21)	11
2.5 Channel 2-2 (Head 2 ; Channel 2: Herzberg, PIN11)	13
2.6 Channel 2-3 (Head 2; Channel 3: Al, MSM15)	15
2.7 Channel 3-1 (Head 3 ; Channel 1: Ly- α , AXUV20A#56)	17
2.8 Channel 3-2 (Head 3 ; Channel 2: Herzberg, PIN12)	19
2.9 Channel 3-3 (Head 3 ; Channel 3: Al, AXUV20B#59)	21
2.10 Lyman- α channels (1-1; 2-1; 3-1)	23
2.11 Herzberg channels (1-2; 2-2; 3-2)	24
2.12 Al channels (1-3; 2-3; 3-3)	25
3 Discussion – Conclusion	27

Reference documents

[RD1] : Final_LYRA_NI_Instrument_Calibration_Plan-V1.1.doc (ROB: 09/03/2006)

[RD2] : LYRA_Assembly_270705.xls (PMOD)

[RD3] : RP-ROB-LYR-0132-NI-July2005



Scope

The purpose of this report is to summarize results from the NI calibration at PTB-Bessy II (2006).

1 Execution Plan for LYRA

For more details, see [RD1]. The PTB campaign plan was executed as following:

Activities number	Activities name	Remark
1	Linearity vs Flux at $\lambda_{1 \text{ or } 2}$	See RD1
2	Stability vs Time at $\lambda_{1 \text{ or } 2}$	“
3	Spectral responsivity [40-240 nm]	“
4	Raster Scan at $\lambda_{1 \text{ or } 2}$	“
5	VIS-Leds testing (On-Off)	“
6	Signal vs Integration time LYRA	“

All tests were performed around 37-38°C (LYRA foot sensor) and measured at **121.6nm** for Ly- α channels (1-1, 2-1 & 3-1), at **210nm** for Herzberg channels (1-2, 2-2 & 3-2) and at **50nm** for Al channels (1-3, 2-3 & 3-3).

The linearity was investigated using different aperture stops or by varying the exit slit of the respective monochromator. For the signal stability, the shutter was opened and closed every 60s (short stability) then every 600s (long). Some “extra” tests were carried out. The expected beam power was calculated using the responsivity data.

The responsivity was measured in the center position at regular intervals and in finest steps close the filter cut-on/off. Voltage units were changed to current units (nA or pA) using the appropriate gain resistor [see RD2]. Corrections for the small decline of the current of the synchrotron storage ring during the time period of each measurement have been applied.

All Leds measurements (stability vs time with Leds on/off) were performed with the new electronics board (IIU). LEDs tests were tried on all Herzberg and Lyman- α channels. You will find the corresponding ranges marked and explained with different colors (UV = UV-LED on, VIS = visible LED on, SR = synchrotron radiation on).



2 RESULTS

2.1 Channel 1-1 (Head 1 ; Channel 1: Ly- α , MSM12)

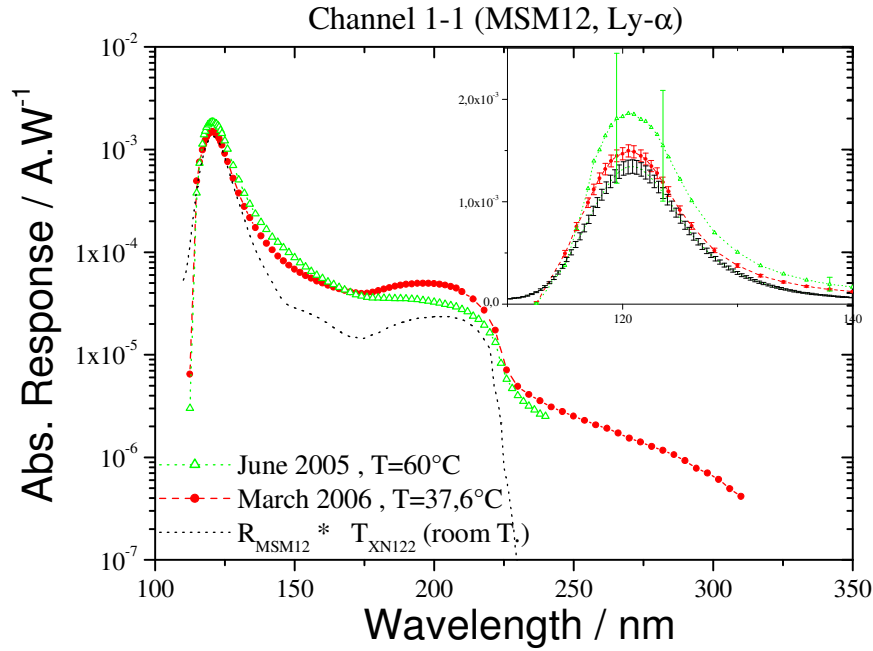


Figure 1. Absolute spectral responsivity (in A/W) of channel 1-1. For comparison, the dotted line represents the model used in the LYRA radiometric model (detector R x Filter T).

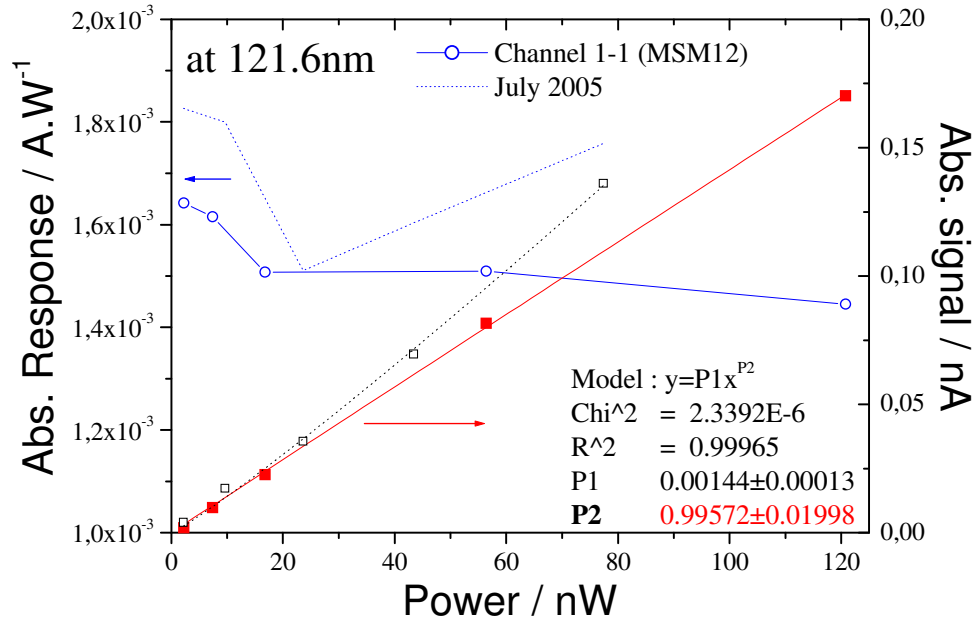


Figure 2. Flux linearity of channel 1-1 (Response & signal vs. incident power) at 121.6nm with the fitted function $I = aP^b$.

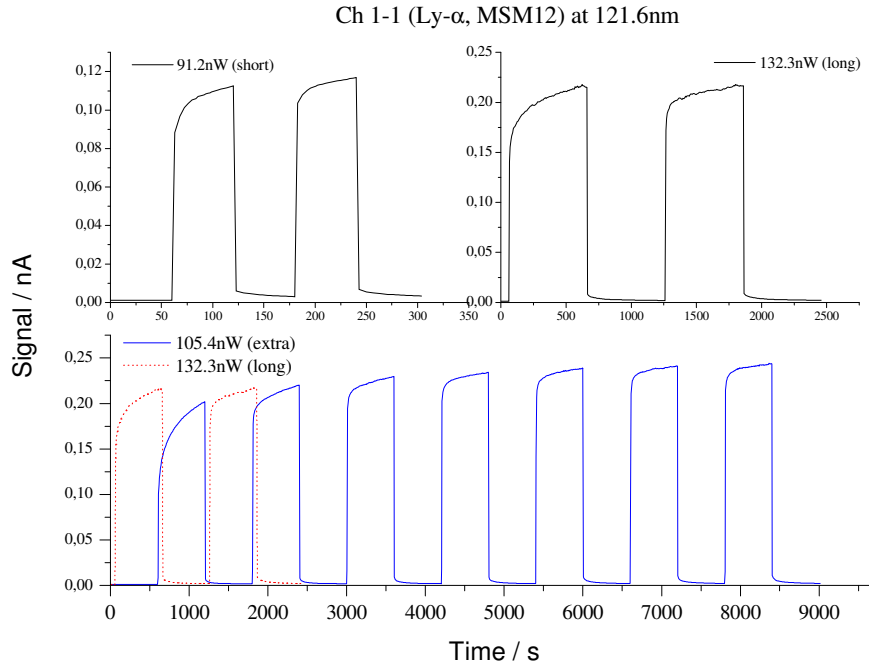


Figure 3. Absolute signal in nano-ampere as a function of time at 121.6 nm.

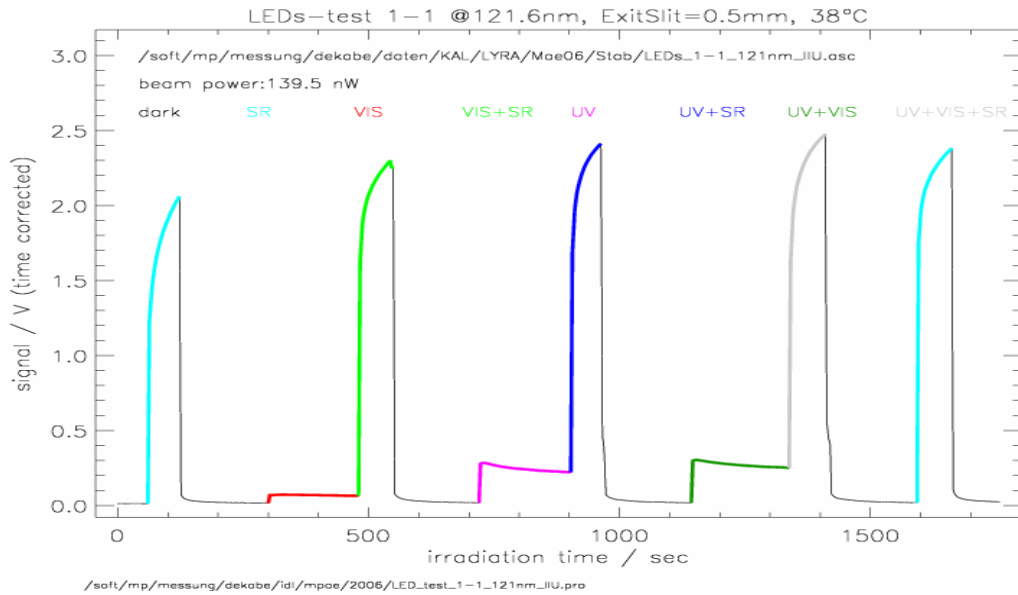


Figure 4. Absolute signal as a function of time at 121.6 nm (38°C) with LEDs light sources (on/off).



2.2 Channel 1-2 (Head 1 ; Channel 2: Herzberg, PIN10)

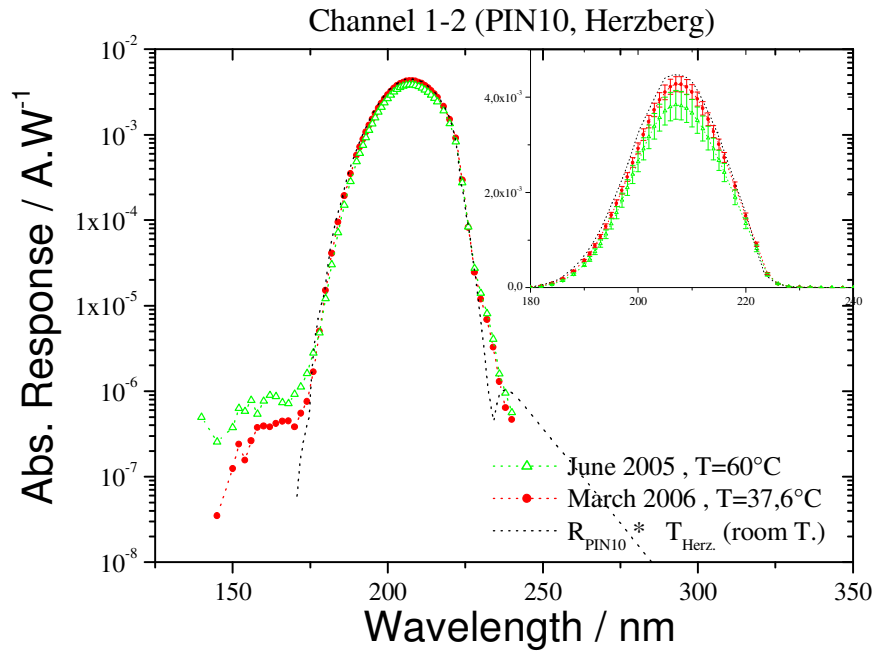


Figure 5. Absolute spectral responsivity (in A/W) of channel 1-2. The inset shows the same in linear scale.

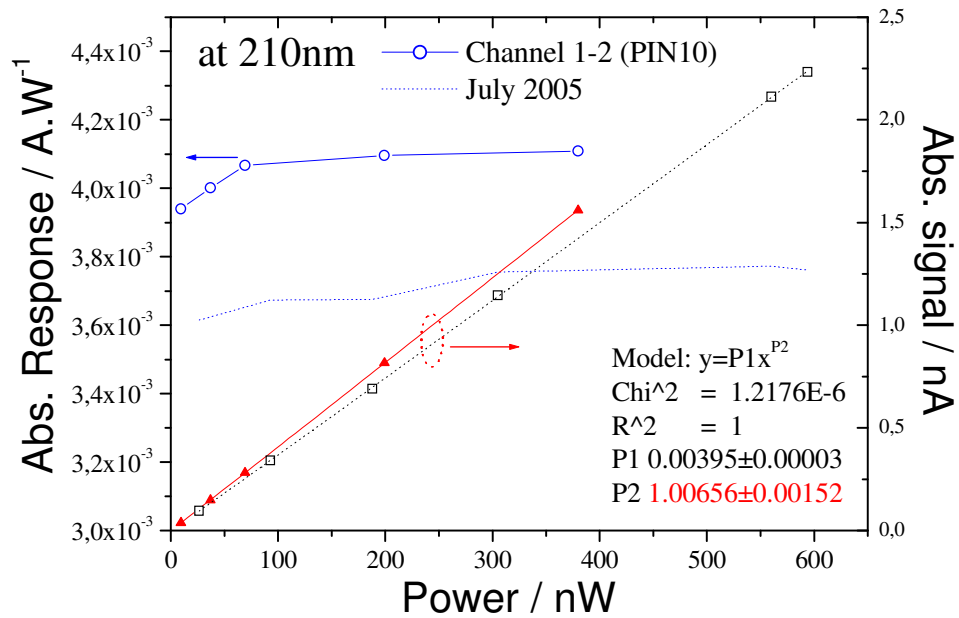


Figure 6. Flux linearity of channel 1-2 (Response & signal vs. incident power) at 210nm with the fitted function $I=aP^b$.

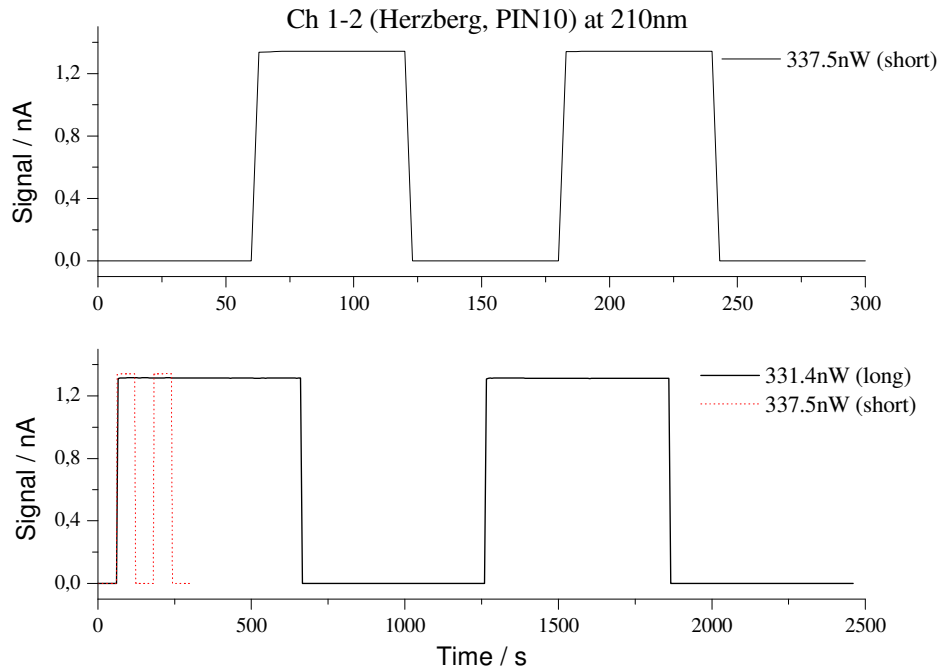


Figure 7. Absolute signal in nano-ampere as a function of time at 210 nm.

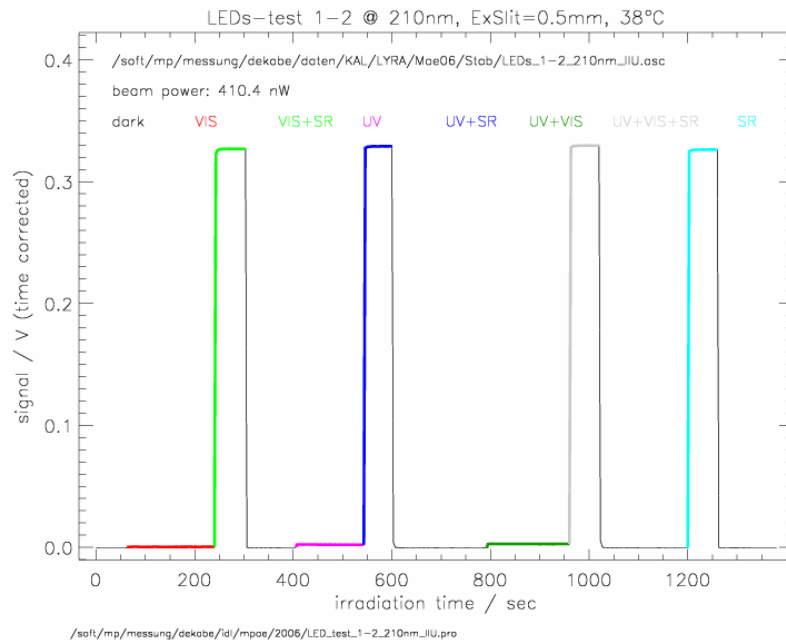


Figure 8. Absolute signal as a function of time at 210 nm (38°C) with LEDs light sources (on/off).



2.3 Channel 1-3 (Head 1 ; Channel 3: Al, MSM11)

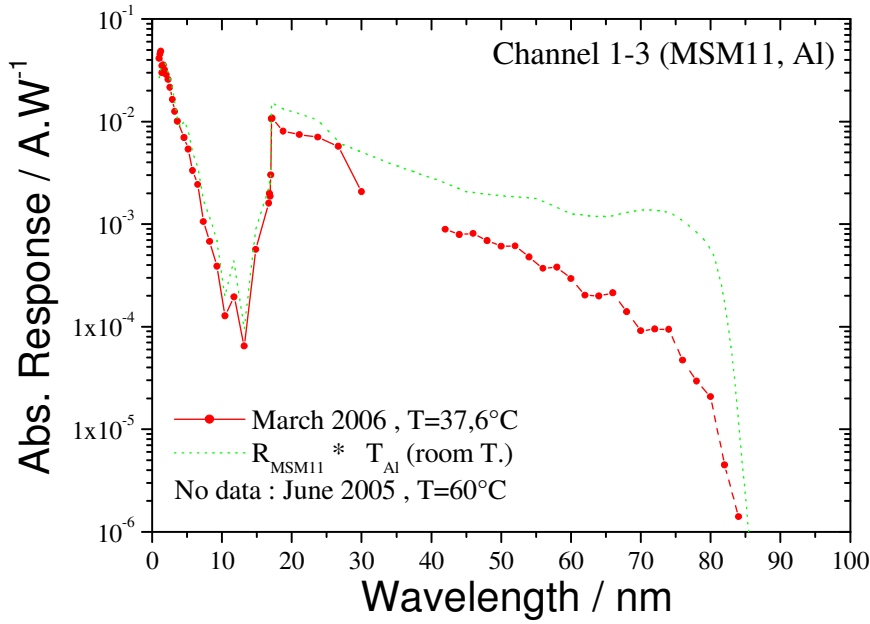


Figure 9. Absolute spectral responsivity (in A/W) of channel 1-3 between 1nm and 80 nm.

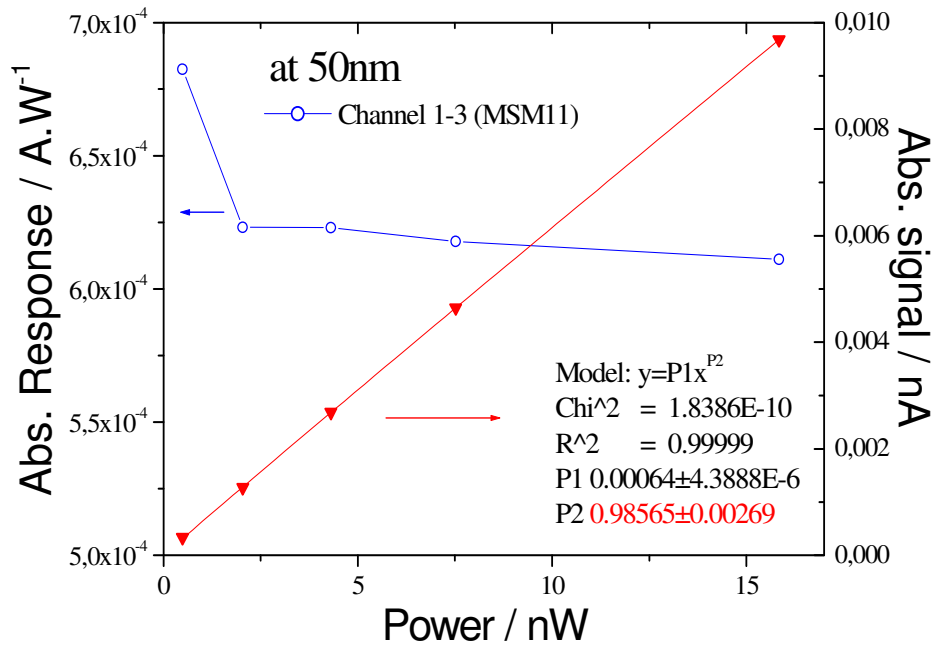


Figure 10. Flux linearity of channel 1-3 (Response & signal vs. incident power) at 50nm with the fitted function $I=aP^b$.

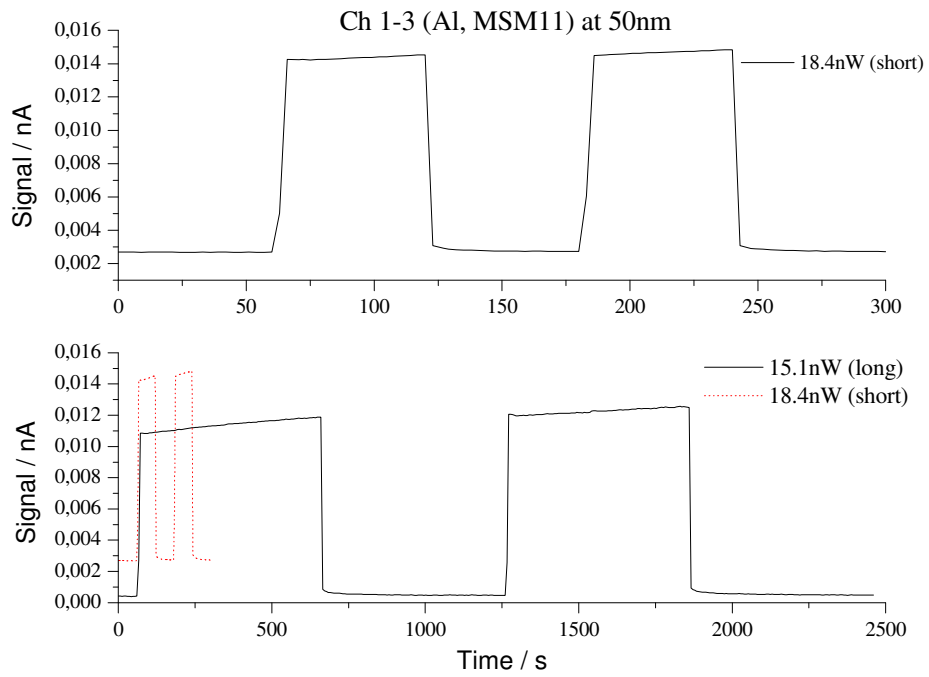


Figure 11. Absolute signal in nano-ampere as a function of time at 50nm.



2.4 Channel 2-1 (Head 2 ; Channel 1: Ly- α , MSM21)

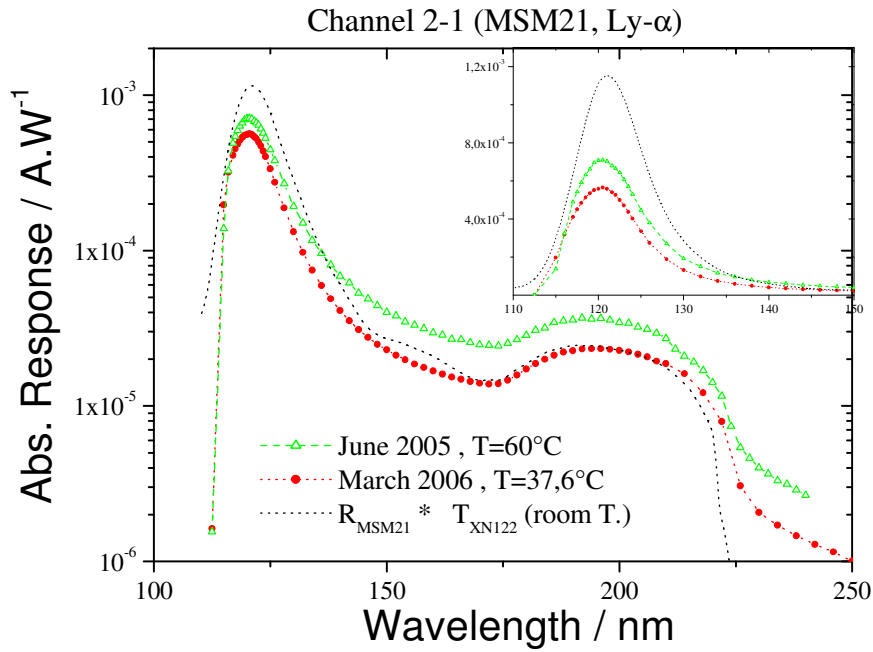


Figure 12. Absolute spectral responsivity (in A/W) of channel 2-1. The inset shows the same in linear scale.

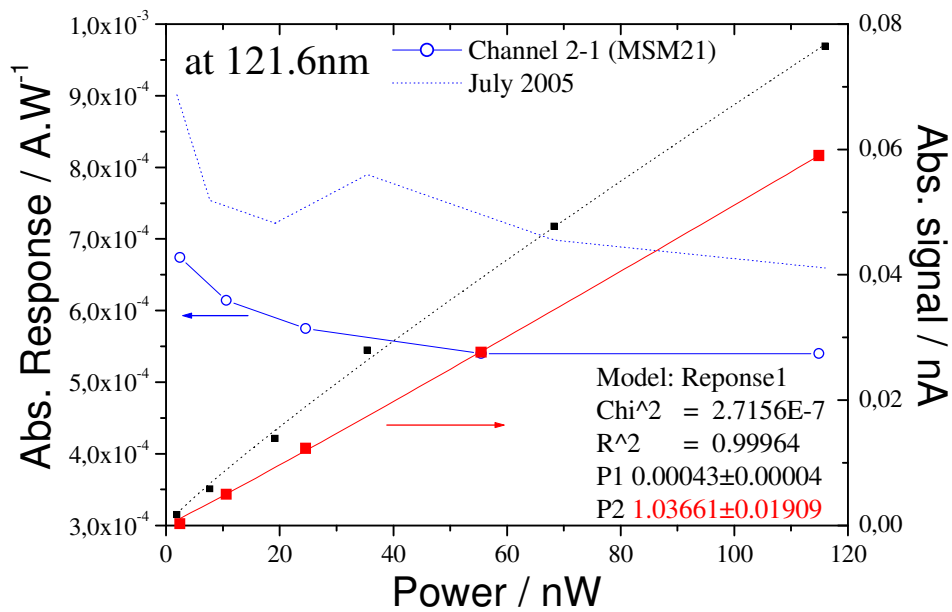


Figure 13. Flux linearity of channel 2-1 (Response & signal vs. incident power) at 121.6nm with the function $I=aP^b$.

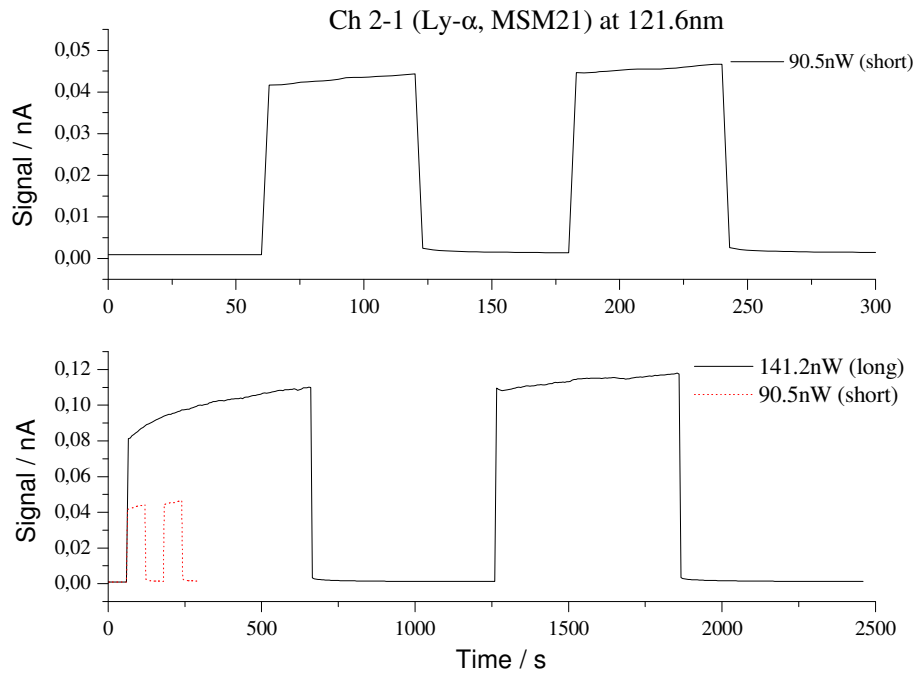


Figure 14. Absolute signal in nano-ampere as a function of time at 121.6 nm.

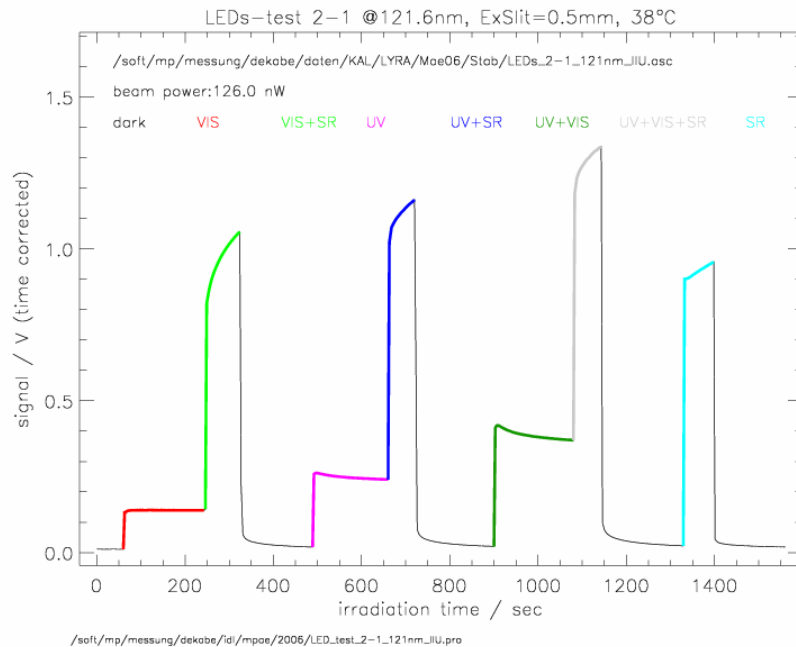


Figure 15. Absolute signal as a function of time at 121.6 nm (38°C) with LEDs light sources (on/off).



2.5 Channel 2-2 (Head 2 ; Channel 2: Herzberg, PIN11)

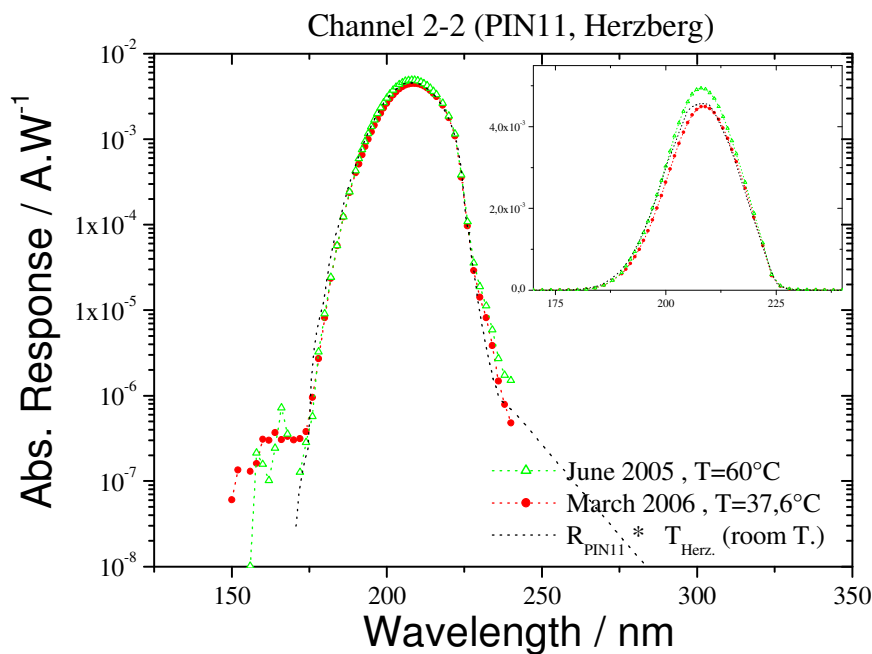


Figure 16. Absolute spectral responsivity (in A/W) of channel 2-2. The inset shows the same in linear scale.

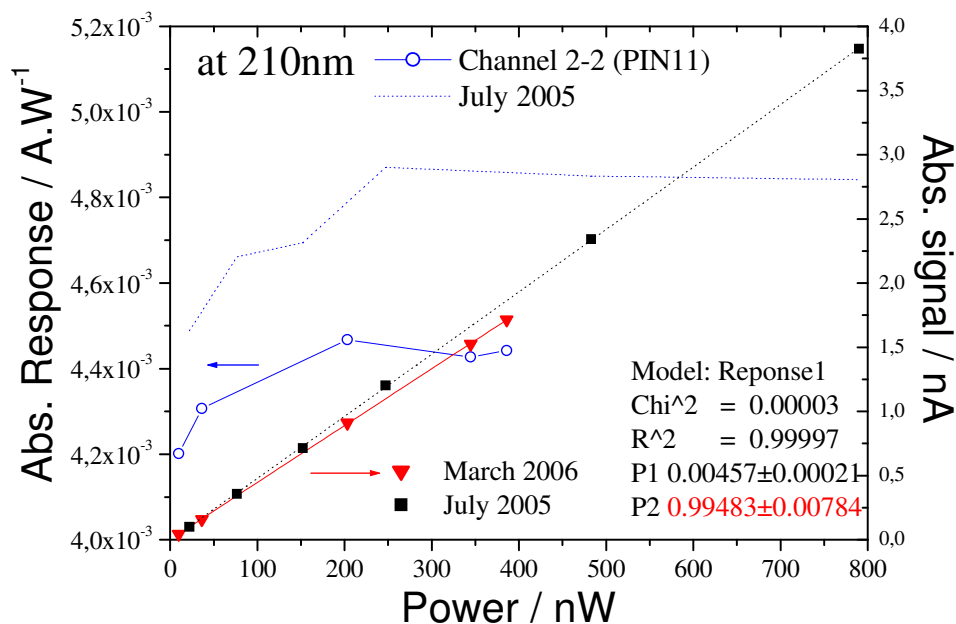


Figure 17. Flux linearity of channel 2-2 (Response & signal vs. incident power) at 210nm with the fitted function $I=aP^b$.

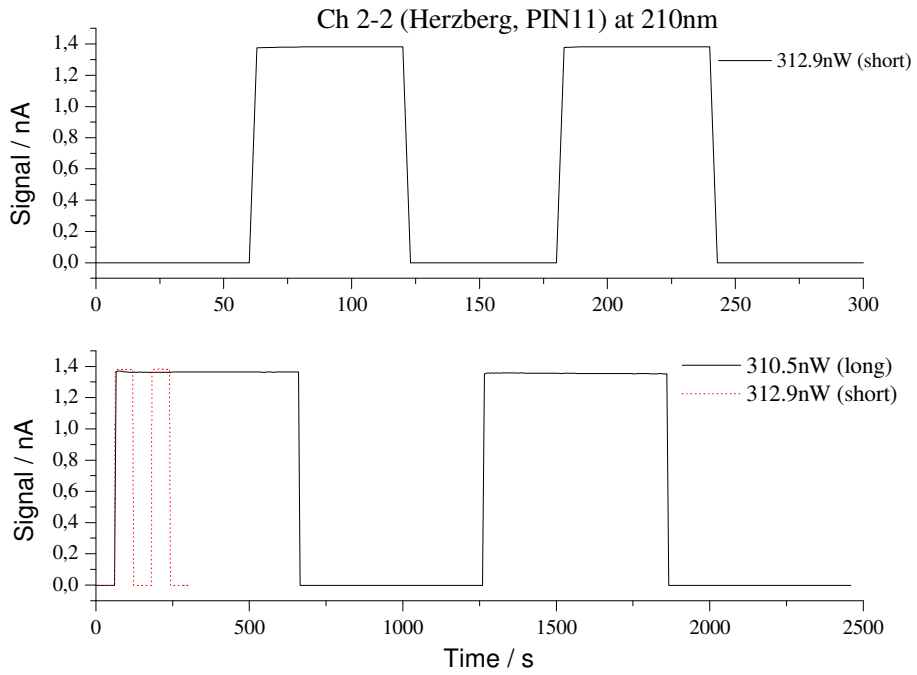


Figure 18. Absolute signal in nano-ampere as a function of time at 210 nm.

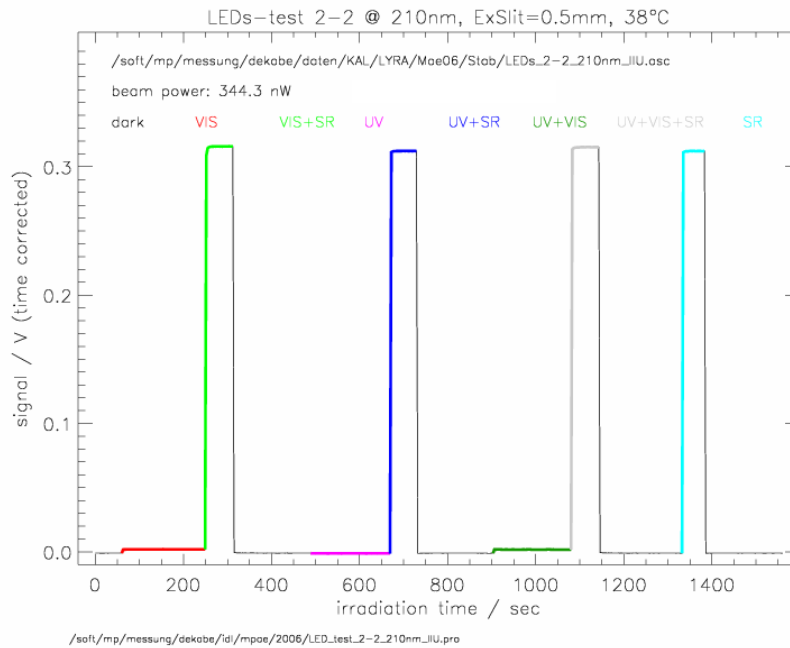


Figure 19. Absolute signal as a function of time at 210 nm (38°C) with LEDs light sources (on/off).



2.6 Channel 2-3 (Head 2; Channel 3: Al, MSM15)

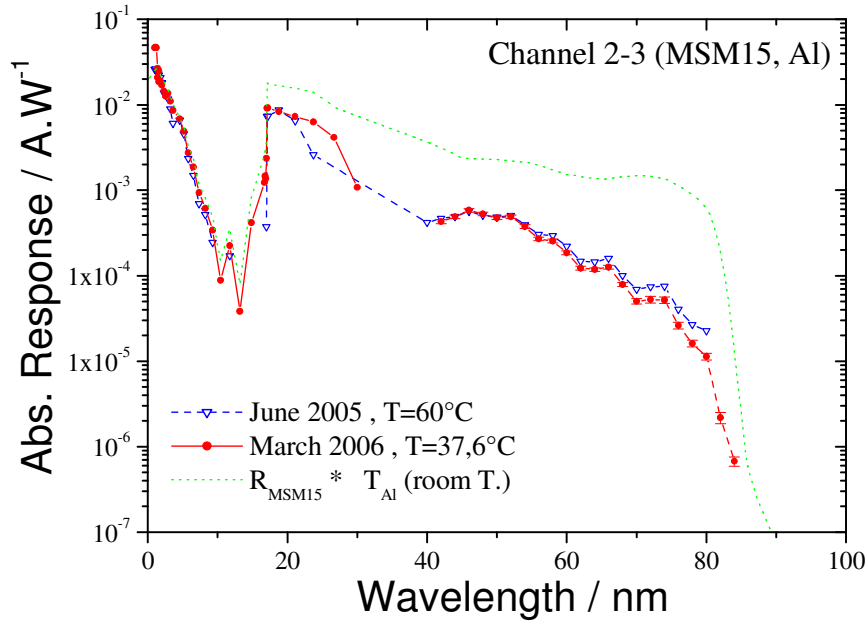


Figure 20. Absolute spectral responsivity (in A/W) of channel 2-3. The inset shows the same in linear scale.

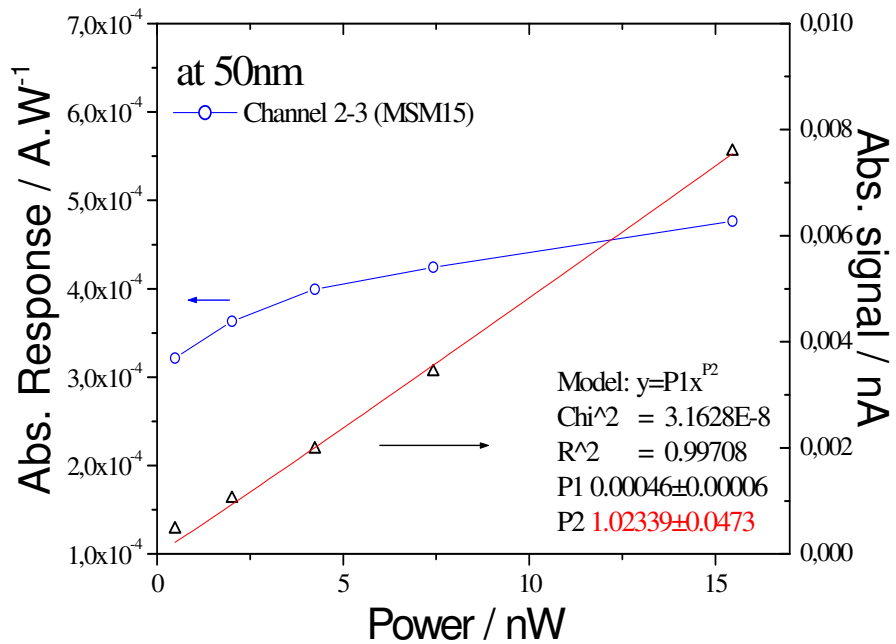


Figure 21. Flux linearity of channel 2-3 (Response & signal vs. incident power) at 50nm with the fitted function $I=aP^b$.

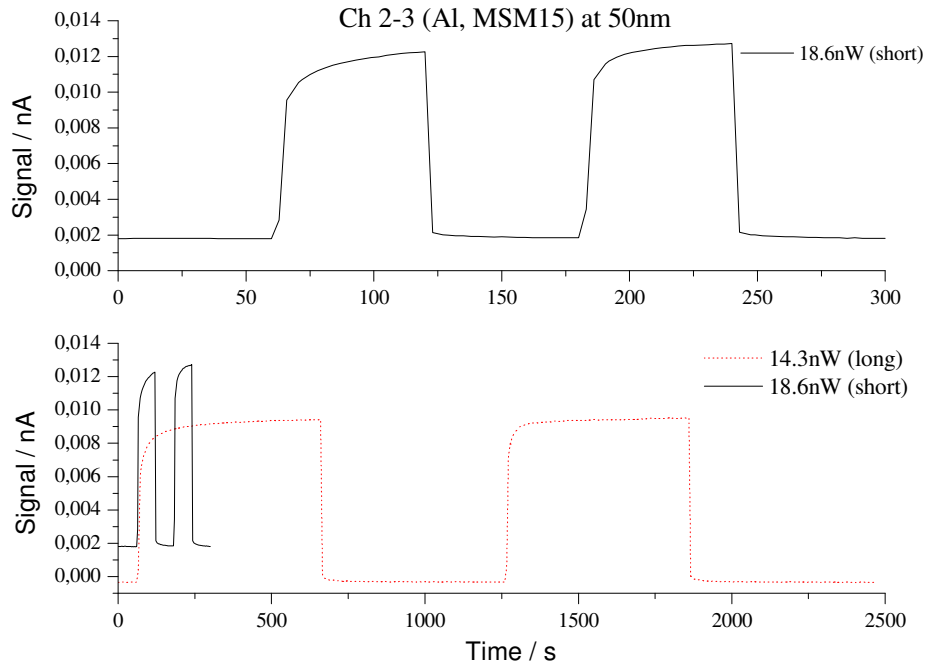


Figure 22. Absolute signal in nano-ampere as a function of time at 50 nm.



2.7 Channel 3-1 (Head 3 ; Channel 1: Ly- α , AXUV20A#56)

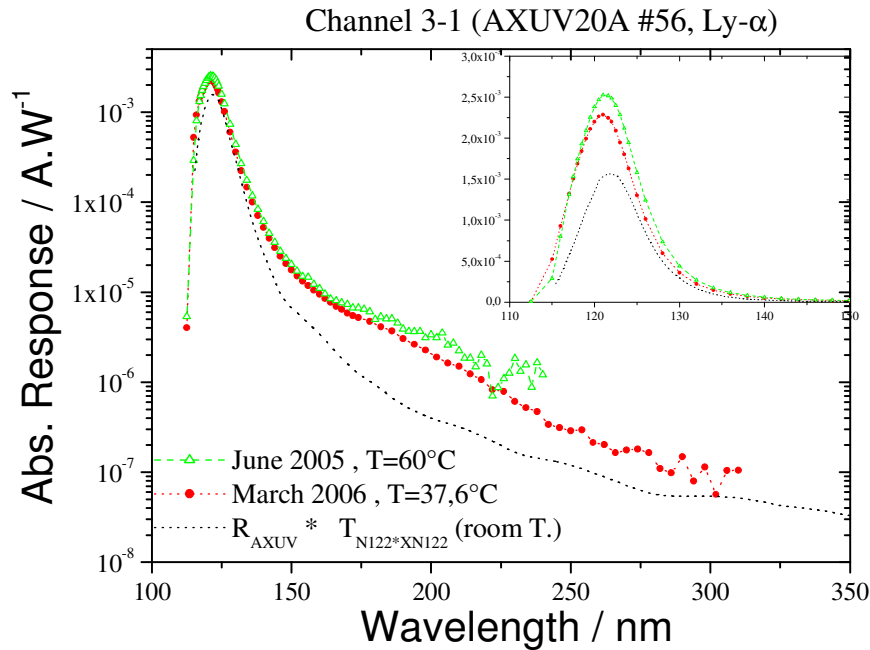


Figure 23. Absolute spectral responsivity (in A/W) of channel 3-1. The inset shows the same in linear scale.

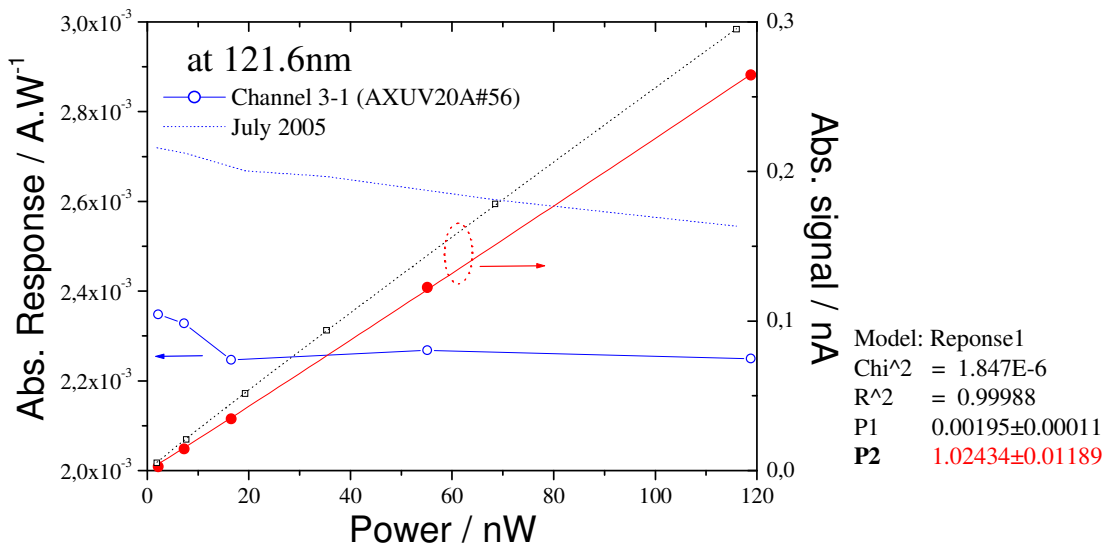


Figure 24. Flux linearity of channel 3-1 (Response & signal vs. incident power) at 121.6nm with the function $I=ap^b$.

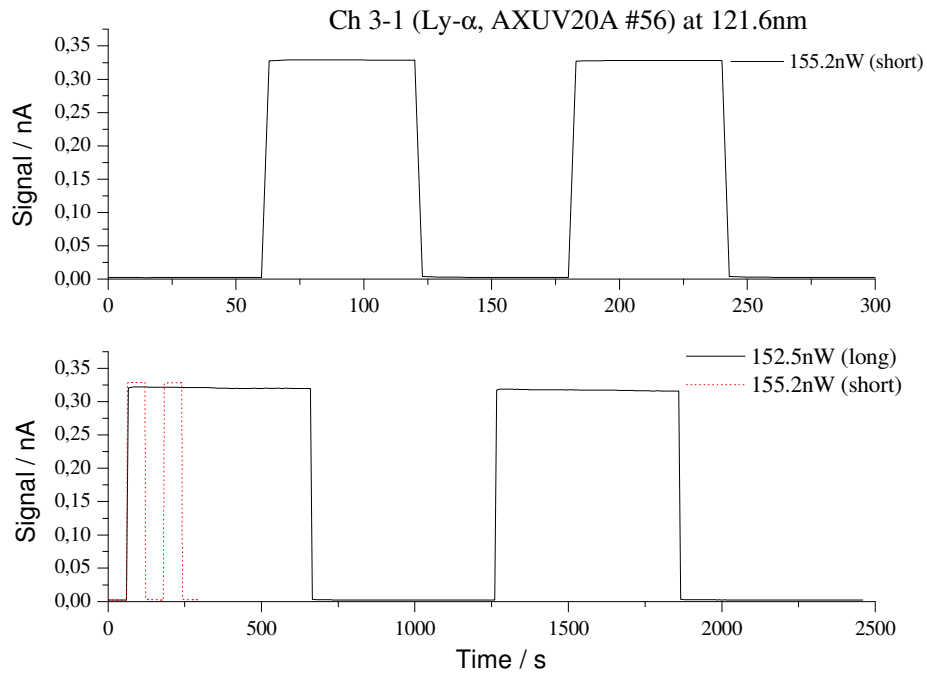


Figure 25. Absolute signal in nano-ampere as a function of time at 121.6 nm.

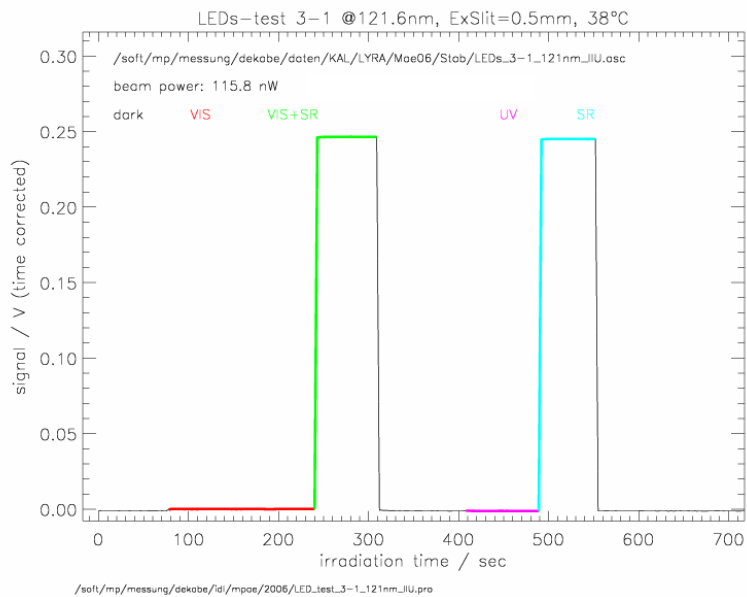


Figure 26. Absolute signal as a function of time at 121.6 nm (38°C) with LEDs light sources (on/off).



2.8 Channel 3-2 (Head 3 ; Channel 2: Herzberg, PIN12)

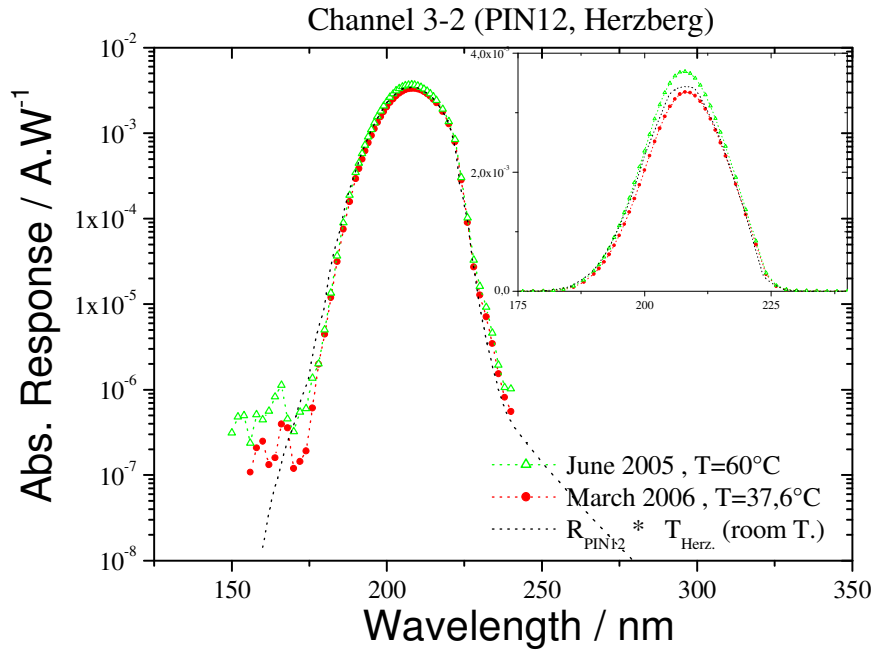


Figure 27. Absolute spectral responsivity (in A/W) of channel 3-2. The inset shows the same in linear scale.

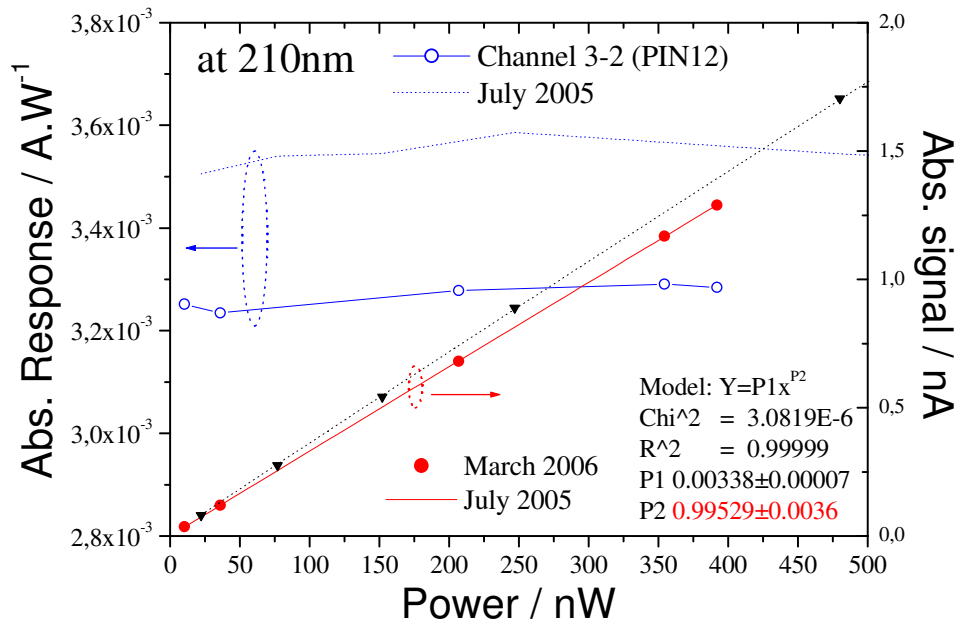


Figure 28. Flux linearity of channel 1-2 (Response & signal vs. incident power) at 210nm with the fitted function $I=aP^b$.

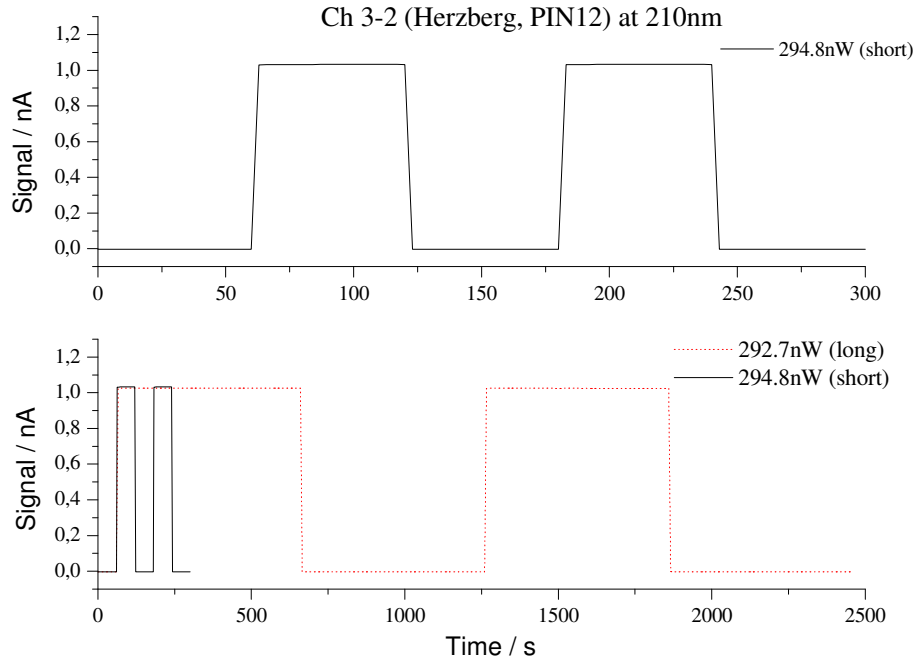


Figure 29. Absolute signal in nano-ampere as a function of time at 210 nm.

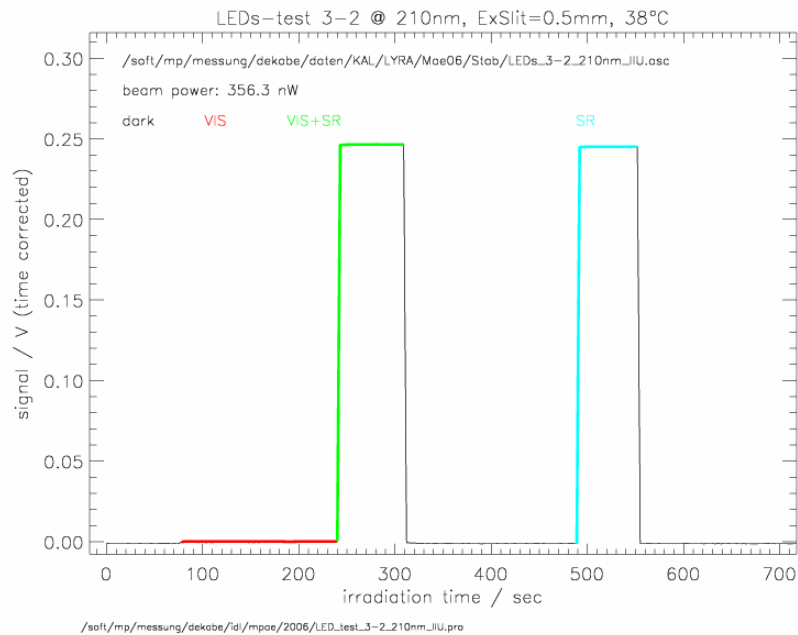


Figure 30. Absolute signal as a function of time at 210 nm (38°C) with LEDs light source (on/off).



2.9 Channel 3-3 (Head 3 ; Channel 3: Al, AXUV20B#59)

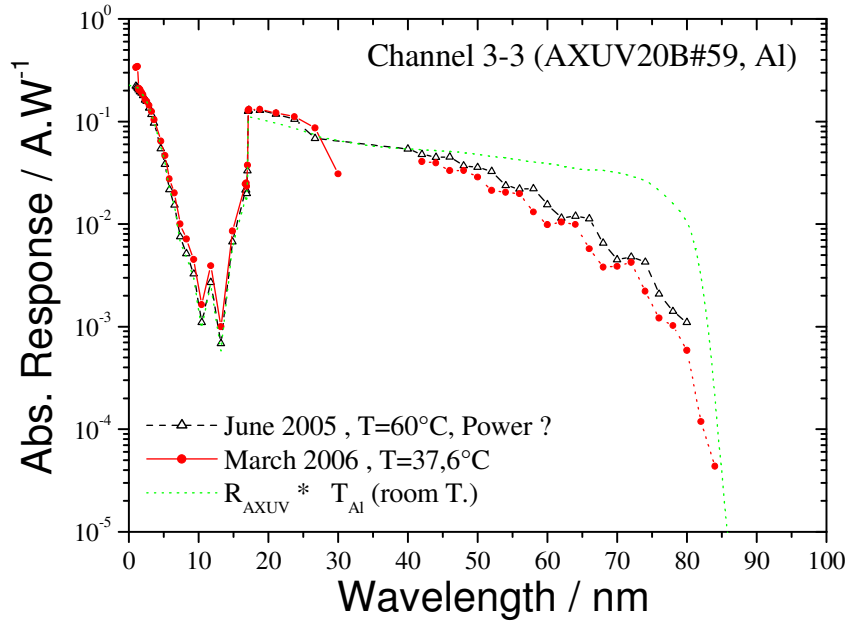


Figure 31. Absolute spectral responsivity (in A/W) of channel 3-3 between 1nm and 84 nm.

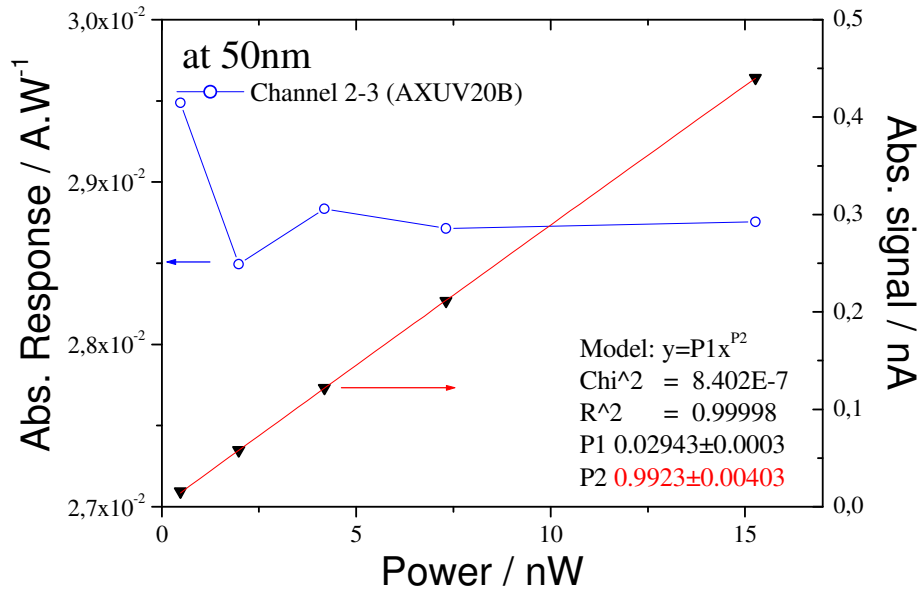


Figure 32. Flux linearity of channel 3-3 (Response & signal vs. incident power) at 50nm with the fitted function $I=aP^b$.

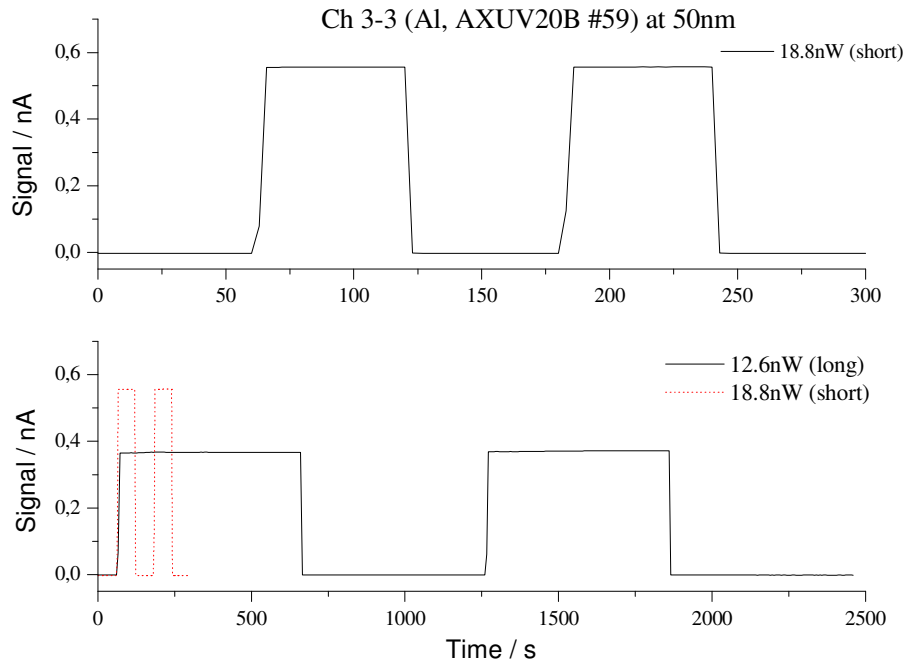


Figure 33. Absolute signal in nano-ampere as a function of time at 50 nm.



2.10 Lyman- α channels (1-1; 2-1; 3-1)

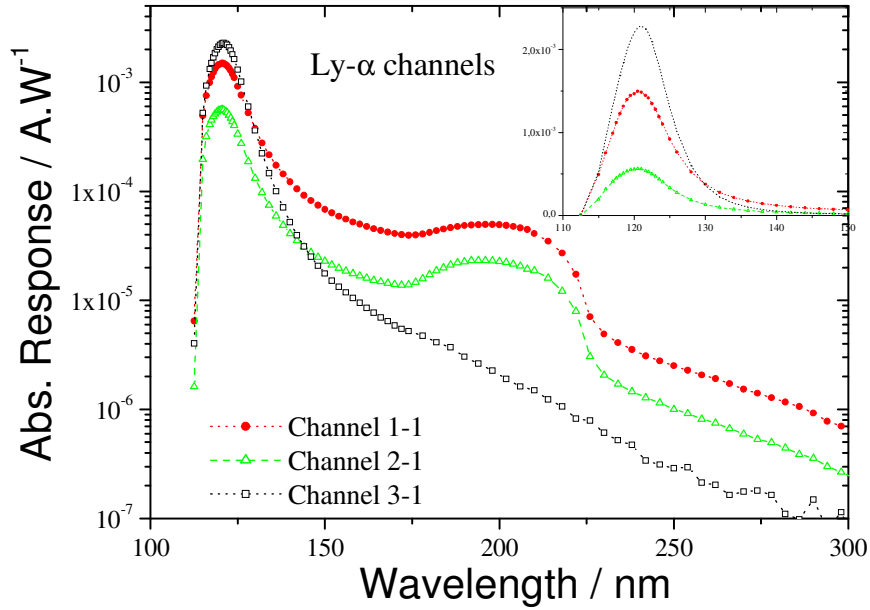


Figure 34. Absolute spectral responsivity (in A/W) of Ly- α channels.

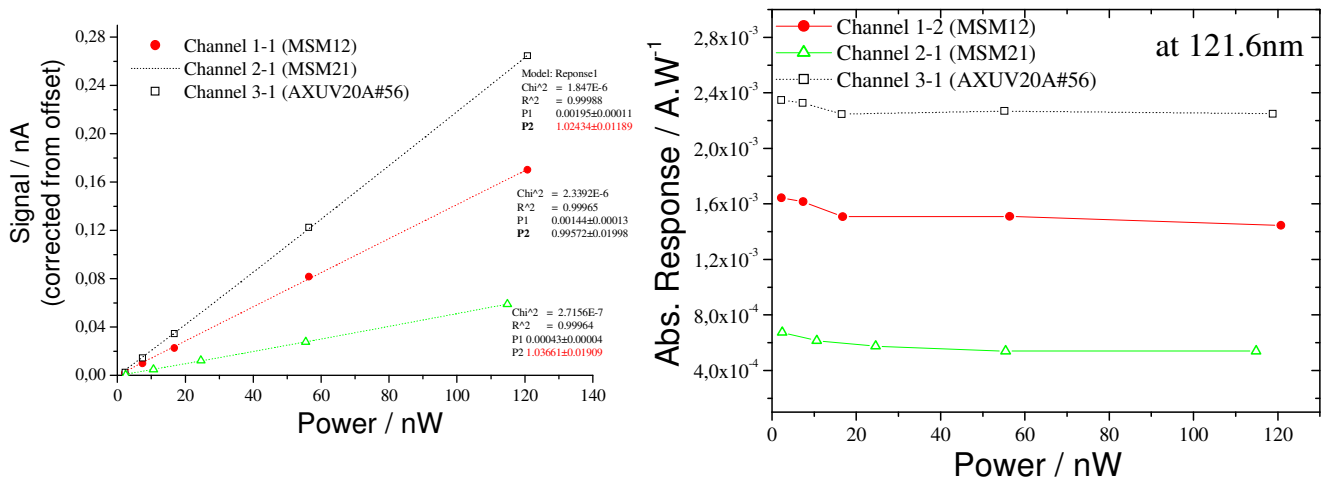


Figure 35. Flux linearity of Ly- α channels (Response & Signal vs. incident power) at 121.6nm.



2.11 Herzberg channels (1-2; 2-2; 3-2)

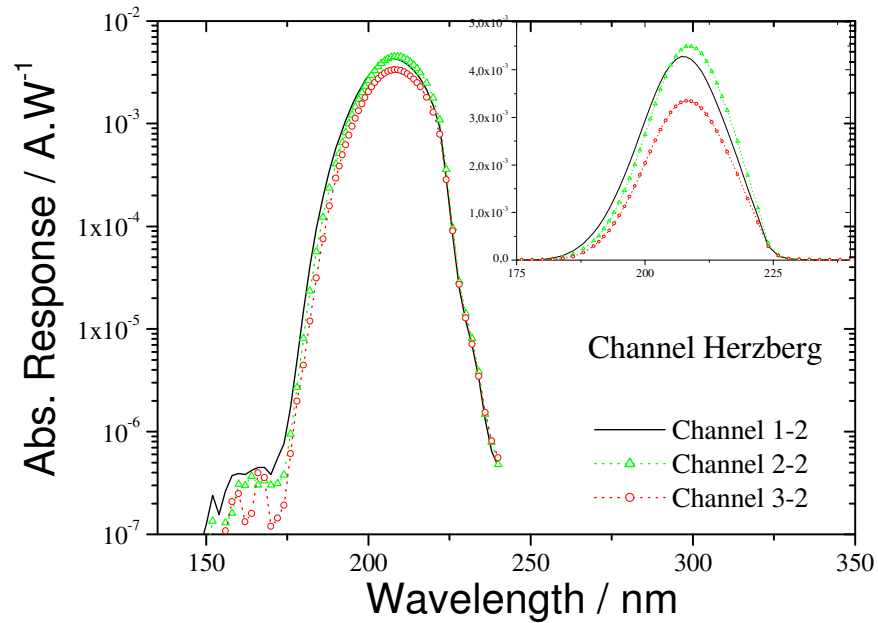


Figure 36. Absolute spectral responsivity (in A/W) of Herzberg channels.

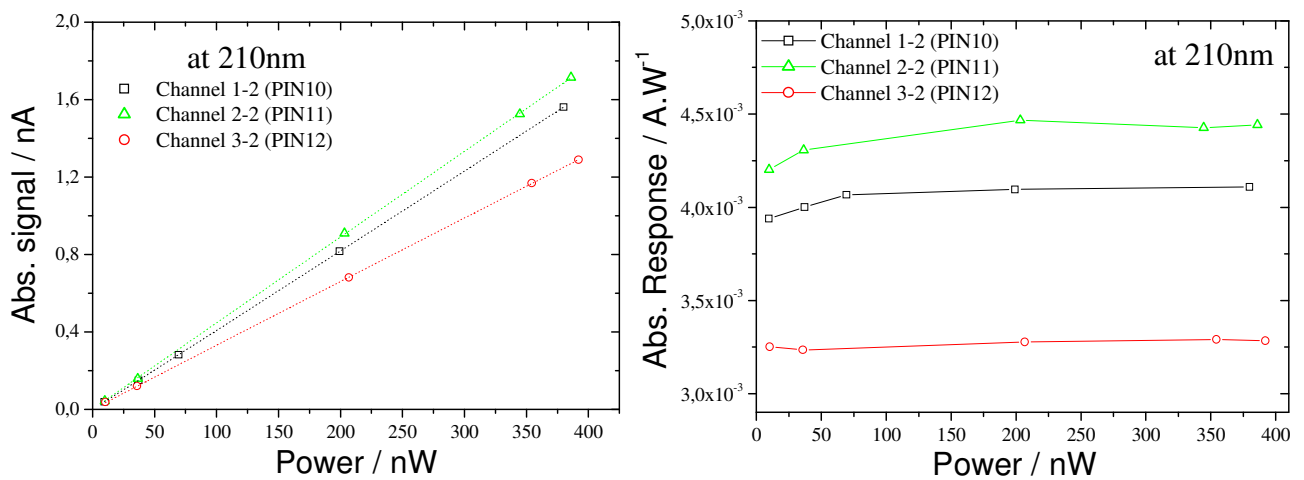


Figure 37. Flux linearity of Herzberg channels (Response & Signal vs. incident power) at 210nm.



2.12 Al channels (1-3; 2-3; 3-3)

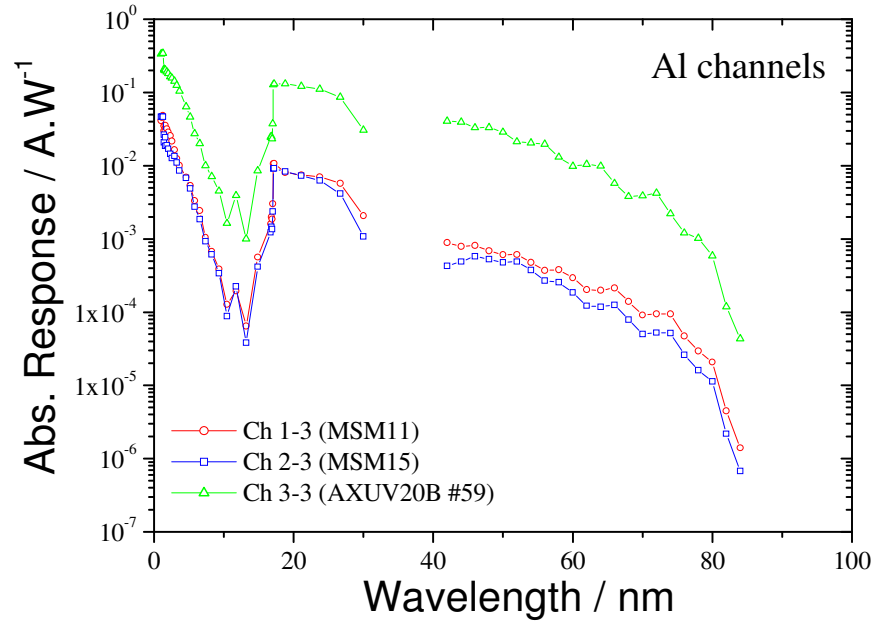


Figure 38. Absolute spectral responsivity (in A/W) of Al channels between 1nm and 84 nm.

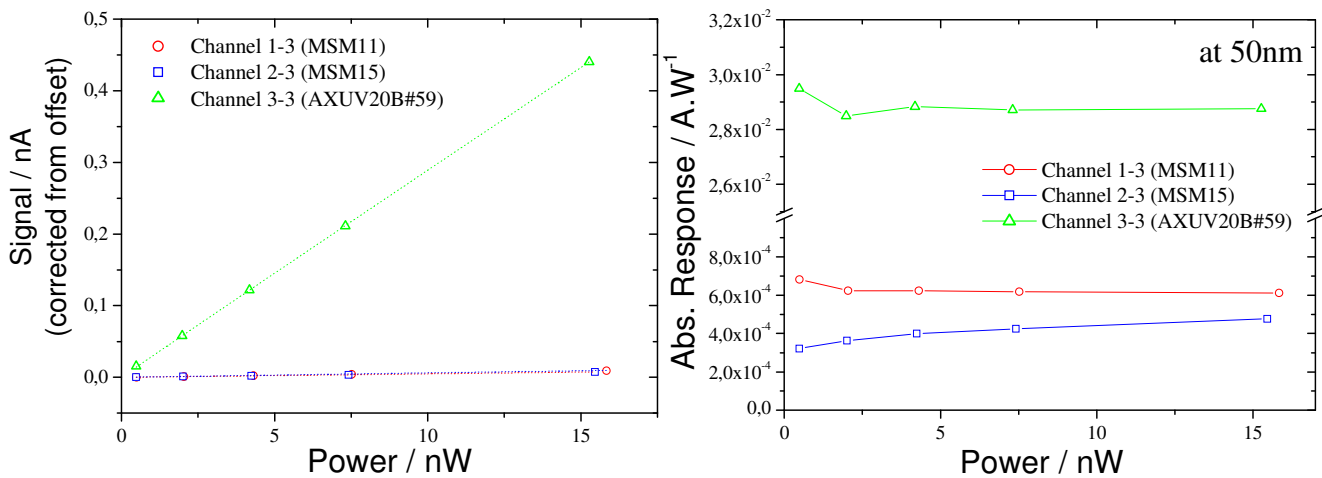


Figure 38. Flux linearity of Al channels (Response & Signal vs. incident power) at 50nm.



Table 1 summarizes the derived results using the TIME-SEE solar spectrums. More information can be found in the updated LYRA radiometric model web site.

http://lyra.oma.be/radiometric_model/radiometric_model.php

Table 1: Expected output signals and purities (width 2.5nm at 121.5nm for Ly- α ; 200-220nm for Herzberg, 1-20nm for Zr and 17-80nm for Al) in LYRA channels for minimum & maximum solar activity conditions.

Expected SIGNAL and Purity			at Solar Min	at Solar Max
HEAD 1	Channel 1	Ly+MSM12	240.5pA [24.4%]	267pA [30.2%]
	Channel 2	Herzb+PIN10	12.565nA [83.3%]	12.587nA [83.2%]
	Channel 3	Al+MSM11	85.9pA [58.3%]	4.945nA [2.5%]
	Channel 4	Zr₃₀₀+AXUV20D	699.2pA [99.8%]	19.091nA [100%]
HEAD 2	Channel 1	Ly+MSM21	103.9pA [21.1%]	113.9pA [26.4%]
	Channel 2	Herzb+PIN11	13.745nA [83.6%]	13.761nA [83.6%]
	Channel 3	Al+MSM15	74.02pA [59.3%]	3.837nA [2.7%]
	Channel 4	Zr₁₅₀+MSM19	94.82pA [99.6%]	2.772nA [100%]
HEAD 3	Channel 1	Ly+AXUV20A	112.54pA [80.6%]	147.55pA [84.3%]
	Channel 2	Herzb+PIN12	10.145nA [83.3%]	10.156nA [83.2%]
	Channel 3	Al+AXUV20B	1.09nA [71.6%]	36.83nA [5.3%]
	Channel 4	Zr₃₀₀+AXUV20C	709.52pA [99.8%]	19.31nA [100%]



Here also we rather have an upper limit since not the entire UV and visible spectrum is taken into account. In blue, the channels with low purity (below 50%). Note that the Zr filter thickness for AXUV channels is 300nm and 150nm for MSM diamond detectors (Head 2, Ch 4).

3 Discussion – Conclusion

For Ly- α channels the spectral response of MSM diamond detectors (Head1Ch1 & Head2Ch1) are lower in the 105-170nm wavelength range than the AXUV- Ly- α channel (Head3Ch1) but higher at around 200-220nm due to the high response of diamond photodetectors (see Fig.34). This result in a lower signal purity, around 21-24% compared to the 80% of the AXUV channel. The other main issue is the instability of MSM channels (large drift) at Ly- α (indeed, at 50nm the MSM looks more stable: cf Fig 22).

For Herzberg channels (Head1Ch2, Head2Ch2, Head3Ch2), the spectral responsivity fit well with the radiometric model and the previous calibration campaign of July 2005 (inside the uncertainty). The expected signal and purity are high (10-13nA; >83%). These PIN channels look stable and linear at around 210nm.

For Al channels (Head1Ch3, Head2Ch3, Head3Ch3), the signal looks stable at 50nm (at least for AXUV-Head3Ch3). Note that there is a large discrepancy with the radiometric model for Al channels due to the rapid decrease of the response at around 40-80nm (cf. Fig 39). For the H3Ch3, the signal purity is around 70% to be compared with 59% for MSM-Al channels (H1Ch3 & H2Ch3).

Checking for holes in the filters of the Al and Zr-channels was done by raster scanning over all 6 channels at 200nm. No channel showed a signal higher than the dark signal (i.e no pinholes).

Stability (signal vs time, integration time vs Leds) will be analysed in detail by ROB (noise fluctuation, SNR) in order to determine the nominal cadence and the choice of the Heads (continuously, weekly, monthly basis). Short term stability with IIU @ 50°C (not shown) will be further analysed.